Metal speciation dynamics in colloidal ligand dispersions.
Part 3: Lability features of steady-state systems

J.P. Pinheiro [a,*], R.F. Domingos [b], M. Minor [c], H.P. van Leeuwen [c]

[a] CBME, Departamento de Química e Bioquímica/FCT, Universidade do Algarve, Campus de Gambelas, 8005-139 Faro, Portugal
[b] CMQA, Departamento de Química e Bioquímica/FCT, Universidade do Algarve, Campus de Gambelas, 8005-139 Faro, Portugal
[c] Laboratory of Physical Chemistry and Colloid Science, Wageningen University, Dreijenplein 6, 6703 HB Wageningen, The Netherlands

Abstract

A lability criterion is developed for dynamic metal binding by colloidal ligands with convective diffusion as the dominant mode of mass transport. Scanned stripping chronopotentiometric measurements of Pb(II) and Cd(II) binding by carboxylated latex core-shell particles were in good agreement with the predicted values. The dynamic features of metal ion binding by these particles illustrate that the conventional approach of assuming a smeared-out homogeneous ligand distribution overestimates the lability of a colloidal ligand system. Due to the nature of the spatial distribution of the binding sites, the change in lability of a metal species with changing ligand concentration depends on whether the ligand concentration is varied via manipulation of the pH (degree of protonation) or via the particle concentration. In the former case the local ligand density varies, whereas in the latter case it is constant. This feature provides a useful diagnostic tool for the presence of geometrically constrained binding sites.
© 2006 Elsevier B.V. All rights reserved.

Keywords: Metal speciation; Colloidal dispersions; Lability; Stripping chronopotentiometry

1. Introduction

In colloidal metal complex systems the spatial distributions of ligand and bound metal are constrained by geometrical and site distribution features of the particles. This feature has important consequences for the dynamic properties of the metal species. For ligands located on the surface of colloidal particles it has already been shown that the dynamic metal speciation features arise from the coupling between the chemical kinetics of complex formation/dissociation and the local diffusion-controlled transport of metal ions to/from the particle [1]. That led us to introduce the concept of 'generalized' rates of association and dissociation for colloidal metal complexes, k_a^* and k_d^*

[1], which may differ by several orders of magnitude from their homogeneous solution counterparts, k_a and k_d. The conventional approach of taking a colloidal ligand dispersion as a smeared-out homogeneous solution [2–4] overestimates both the dynamics and the lability of the colloidal metal complexes.

Colloidal ligands are typical components of natural waters [5] and electrochemical techniques have been extensively applied to metal speciation analysis in such media [6]. We have proposed electrochemical lability criteria for colloidal metal species under conditions where diffusion is the dominant mode of mass transport [7], such as in direct voltammetry of non-stirred solutions. However, due to their lower detection limit, stripping voltammetric techniques are usually preferred over direct methods for speciation analysis of natural waters [6]. During the deposition step of stripping methods, which is the decisive one for speciation analysis, the solution is usually stirred, and thus convective diffusion is the relevant mode of mass transport.

* Corresponding author. Tel.: +351 289 800905; fax: +351 289 800066.
E-mail address: jpinhei@ualg.pt (J.P. Pinheiro).

Nomenclature

Symbols

a	radius of the colloidal particle, m
A	electrode surface area, m^2
C_i	coarse grained concentration of species i, mol m^{-3}
C_i^*	coarse grained concentration of species i in the bulk, mol m^{-3}
$C_{M,T}^*$	total metal coarse grained concentration in the bulk, mol m^{-3}
c_M^*	concentration of the metal in the bulk, mol m^{-3}
$c_{M^0}^*$	concentration of the reduced metal in the bulk of the mercury drop, mol m^{-3}
c_L	concentration of the ligand, mol m^{-3}
c_p	particle number concentration in the volume V, m^{-3}
D_i	diffusion coefficient of the species i in solution, m^2 s^{-1}
$\overline{D}$	mean diffusion coefficient, m^2 s^{-1}
d	thickness of the ligand layer in the colloidal particle, m
$\bar{d}$	thickness of the diffusion layer for a spherical electrode in the presence of complexing ligands, m
$E_{d,1/2}$	half-wave potential for SSCP curve, V
E_d	deposition potential, V
F	Faraday constant, C mol^{-1}
I_d^*	limiting deposition current, A
I_s	stripping current, A
J^*	limiting metal flux into the electrode, mol m^{-2} s^{-1}
J_{dif}^*	maximum diffusive flux, mol m^{-2} s^{-1}
J_{kin}	local kinetic flux, mol m^{-2} s^{-1}
K	complexation constant, mol^{-1} m^3
K'	$=Kc_{L,T}$
k_a	association rate constant of the complex ML, mol^{-1} m^3 s^{-1}

k_a'	$=k_a'c_{L,T}$, s^{-1}
k_a^*	generalized association rate constant of the complex ML, mol^{-1} m^3 s^{-1}
k_d	dissociation rate constant of the complex ML, s^{-1}
k_d^*	generalized dissociation rate constant of the complex ML, s^{-1}
K_{os}	stability constant for outer-sphere complexes, mol^{-1} m^3
k_{-w}	water loss rate constant, s^{-1}
L	lability criterion
L^*	lability criterion for the dynamic colloidal dispersion
L^h	lability criterion for the homogeneous case (Eigen mechanism)
n	number of electrons involved in the faradaic process
r_0	radius of the electrode, m
t	time, s

Greek symbols

α	parameter related to the hydrodynamic nature of the mass transport in the system
δ	thickness of the diffusion layer at the consuming surface, m
$\bar{\delta}$	average of thickness of the diffusion layer, m
ε	ratio of the diffusion coefficients of bound and free metal
γ	constant fraction of δ, independent of D^α
Γ_L	surface ligand concentration, mol m^{-2}
μ	reaction layer thickness, m
τ	transition (stripping) time, s
τ_M^*	limiting transition time in the absence of complexing ligands, s
τ_{M+L}^*	limiting transition time in the presence of complexing ligands, s

Stripping chronopotentiometry (SCP) is a technique that is relatively insensitive to organic adsorption interferences [8,9] while having a detection limit comparable to that of pulsed stripping voltammetries. Even more relevant here is that for the complete depletion mode of scanned stripping chronopotentiometry (SSCP) [10] a known rigorous equation is available for the full wave in the kinetic current regime [11]. Using this expression we demonstrated that the characteristic parameters of the SSCP wave (the limiting wave height, τ^*, and the half-wave deposition potential, $\Delta E_{d,1/2}$) provide an indicator of changes in lability of metal complex systems [12].

The objective of the present work is to extend the dynamic theory for colloidal metal complexes with a lability criterion for a steady-state situation in which convective diffusion is the dominant mode of mass transport. Support-

ing experimental evidence is provided by SSCP measurements of Pb(II) and Cd(II) complexation in dispersions of carboxylated latex particles.

2. Theory

2.1. Dynamic speciation of colloidal metal complexes

Let us consider a homodisperse colloidal ligand dispersion with spherical particles of radius a, where the ligand groups are located in a thin outer shell of thickness d ($d \ll a$). This picture applies to, e.g., synthetic core-shell colloids and to humic matter adsorbed at the surface of solid particles in natural waters. If the thickness of the ligand layer is indeed much smaller than the particle size we can integrate the ligand concentration over the shell

volume and express the result in terms of an equivalent surface concentration, Γ_L [1]

$$\int_a^{a+d} c_L 4\pi r^2 \, dr = \Gamma_{L/A} \tag{1}$$

We further consider a metal ion M that can (i) associate with a binding site, L, in the shell, to generate a colloidal complex, ML and (ii) be reduced to metal atoms M^0 at an electrode

$$\begin{array}{c} M + L \left| \begin{array}{c} k_a^* \\ \rightleftarrows \\ k_d^* \end{array} \right. ML \left. \right| \\ ne^- \updownarrow \\ M^0 \end{array} \tag{2}$$

The overall particle radius $(a + d)$ will be assumed to be small compared with the thickness of the macroscopic diffusion layer thickness, δ, developed at the electrode/dispersion interface. Hence the metal ion concentration gradient is immaterial on the size scale of an individual particle. The apparent rate constants of complex formation and dissociation in colloidal ligand dispersions, k_a^* and k_d^*, are related to the k_a and k_d in a homogeneous solution by [1]:

$$k_a^{*'} = k_a' / \left(1 + k_a' (4\pi a D_M c_p)^{-1} \right) \tag{3a}$$

$$k_d^* = k_d / \left(1 + k_a' (4\pi a D_M c_p)^{-1} \right) \tag{3b}$$

where D_M is the diffusion coefficient of the metal and c_p is the particle number density. The $k_a^{*'}$ and k_a' are useful under conditions of excess of ligand

$$k_a^{*'} = k_a^* C_L \quad \text{and} \quad K' = k_a^{*'} / k_d^* = K C_L \tag{4}$$

where K is the stability constant of the colloidal complex ML and C_L is the smeared-out total ligand concentration [1]. Other symbols have their usual meaning. The association rate constant, k_a, is usually consistent with a mechanism in which formation of an outer-sphere complex between the metal and the ligand, with an electrostatically determined stability constant (K_{os}), is followed by a rate-limiting removal of water from the inner coordination sphere of the metal (k_{-w}), commonly known as the Eigen mechanism [13].

For a colloidal ligand dispersion, the apparent rate constants, $k_a^{*'}$ and k_d^*, have two limiting values:

(i) a kinetic limit for $k_a'(4\pi a D_M c_p)^{-1} \ll 1$, at which $k_a^{*'} = k_a'$ and $k_d^* = k_d$. This situation occurs for metals with relatively low formation rate constants (low k_{-w}) and/or systems with small particles,

(ii) a diffusive limit for $k_a'(4\pi a D_M c_p)^{-1} \gg 1$, at which $k_a^{*'} = 4\pi a D_M c_p$ and $k_d^* = 4\pi a D_M c_p / K'$, respectively. This limit is expected for metals with relatively high k_{-w} values and/or relatively large colloidal particles.

Following the concepts established for homogeneous solutions [14], a metal complex system is denoted as dynamic if the apparent rates of the complex formation/ dissociation reactions are fast on the experimental time scale, t, i.e.,

$$k_a^{*'} t, \ k_d^* t \gg 1 \quad \text{dynamic} \tag{5}$$

If condition (5) is met then equilibrium is fully maintained in the bulk *volume* of the system. At the other extreme, a system for which $k_a^{*'} t, \ k_d^* t \ll 1$ is denoted as static (inert).

In the presence of an ongoing interfacial process, e.g., consumption of M at an electrode surface, the overall flux of M towards the electrode is simultaneously determined by the diffusion and kinetics of interconversion between M and its complex species in the system. The contribution of complexes to the metal flux depends on the relative magnitudes of the diffusive and kinetic fluxes, J_{dif}^* and J_{kin}^*, respectively. The lability criterion, L, is defined as the ratio J_{kin}^* / J_{dif}^*. The well-known limits for dynamic systems are labile (diffusion control) and non-labile (kinetic control) [14]

$$L = J_{kin}^* / J_{dif}^* \begin{cases} \gg 1 & \text{labile} \\ \ll 1 & \text{non-labile} \end{cases} \tag{6}$$

2.2. Dynamic information obtained by SSCP

SSCP is a useful tool to obtain dynamic metal speciation information because the analytical signal (the transition time, τ) always reflects the magnitude of the original deposition flux, irrespective of its nature (i.e., diffusion-controlled or kinetically controlled). The thermodynamic complex stability constant, K, can be calculated from the shift in the half-wave deposition potential, $\Delta E_{d,1/2}$, (analogous to the DeFord–Hume expression) irrespective of the degree of lability of the system [12]

$$\ln(1 + K') = -(nF/RT)\Delta E_{d,1/2} - \ln(\tau_{M+L}^* / \tau_M^*) \tag{7}$$

where τ_{M+L}^* and τ_M^* denote the τ values for limiting deposition current conditions in the presence and in the absence of ligand, respectively.

In colloidal ligand systems, a lower amount of reduced metal and thus a lower τ value generally arises from the reduced diffusion coefficient of the colloidal ML species. Further reduction of τ results if the colloidal complex is not fully labile. A decrease in $c_{M^0}^*$ shifts the SSCP wave to more positive potentials due to the effect of lower $c_{M^0}^*$ on E_{eq} at $t = 0$ [15]. Thus any decrease in τ due to the presence of complexing ligands concomitantly increases $E_{d,1/2}$, (i.e., reduces the negative potential shift) and a consistent relationship is maintained between $E_{d,1/2}$ and K (Eq. (7)).

For quasi-labile or non-labile complexes the apparent association rate constant $k_a^{*'}$ can be calculated from the limiting τ (i.e., τ^*) using the known expression for the thickness of the pertaining reaction layer, μ [16]

$$\mu = (D_M / k_a^{*'})^{1/2} \tag{8}$$

For a known D_{ML}, μ can be obtained from the change in τ^* due to the presence of complexing ligands

$$\tau^*_{M+L}/\tau^*_M = \left[D_M(1+K')/d_M \left((\bar{d}-\mu)/\overline{D}(1+K') + \mu/D_M \right)^{-1} \right] \tag{9}$$

where d_M and $\bar{d}$ are the thicknesses of the diffusion layer for a spherical electrode (for instance a static mercury drop electrode) in the absence and presence of complexing ligands, respectively,

$$d_M = (1/\delta_M + 1/r_0)^{-1} \tag{10a}$$
$$\bar{d} = (1/\bar{\delta} + 1/r_0)^{-1} \tag{10b}$$

with $\bar{\delta}$ and δ_M representing the thickness of the macroscopic diffusion layer in the presence and absence of complexing ligands, and r_0 is the electrode radius. In passing we note that the above reasoning is valid for microelectrodes as long as the condition $(a + d) \ll r_0$ is satisfied. The diffusion layer thicknesses, d_M and $\bar{d}$, are determined by the hydrodynamic conditions prevailing in the deposition step, and depend on the diffusion coefficient according to some power function D^α of the type

$$\delta_i = \gamma D_i^\alpha \tag{11}$$

where α is related to the hydrodynamic nature of the mass transport and varies from 1/2 for pure diffusion conditions to 1/3 for laminar convective diffusion [17] and γ is a constant.

$\overline{D}$ is the average diffusion coefficient that describes the coupled diffusion of complex and free metal under labile conditions [3]

$$\overline{D} = (D_M C_M + D_{ML} C_{ML})/(C_M + C_{ML})$$
$$= D_M(1 + \varepsilon K')/(1 + K') \tag{12}$$

3. Experimental

3.1. Reagents

All solutions were prepared in ultrapure water from a MilliQ Simplicity (resistivity > 18 MΩ cm). Cd(II) stock solution was prepared from solid Cd(NO$_3$)$_2$ (Merck, p.a.), Pb(II) stock solution was prepared from dilution of a lead standard solution (1000 mg/L Merck), and NaNO$_3$ stock solution was prepared from the solid (Merck, suprapur). Stock solutions of MES (2-(N-morpholino) ethanesulfonic acid) and MOPS (3-(N-morpholino)-propanesulfonic acid) buffers were prepared from the solids (Fluka, Microselect, >99.5%). HNO$_3$ (Merck, suprapur) and NaOH (solid from Riedel-de Haën) solutions were used to adjust the pH. Stock dispersions of carboxylated latex nanospheres (10% (w/w)) were obtained from Bangs Labs (US): $(a + d) = 15$ nm, $c_{L,t} = 6.50 \times 10^{-5}$ mol COOH per gram and from Ikerlat Polymers (Spain): $(a + d) = 40.0$ nm, $c_{L,t} = 5.2 \times 10^{-5}$ mol COOH per gram; $(a + d) =$

60.5 nm, $c_{L,t} = 5.1 \times 10^{-5}$ mol COOH per gram and $(a + d) = 129$ nm $c_{L,t} = 5.9 \times 10^{-5}$ mol COOH per gram. The latex particle density is 1.06×10^3 kg m^{-3} and the maximum surface ligand concentration is 3.5×10^{-7} mol m^{-2} for the 15 nm radius particles, 7.3×10^{-7} mol m^{-2} for the 40 nm, 1.1×10^{-6} mol m^{-2} for the 60.5 nm and 2.7×10^{-6} mol m^{-2} for the 129 nm. The 15 nm nanospheres were cleaned to eliminate surfactant by a mixed bed resin method [18] while the others were cleaned by the manufacturer. An ionic strength of 0.01 M was used in all experiments. Voltammetric experiments were performed using particle concentrations between 0.1% and 0.4% (w/w) and Pb(II) and Cd(II) concentrations from 2.0 to 8.0×10^{-7} M. For the 15 nm particles a potentiometric titration was performed to determine the degree of deprotonation at each pH, while the other particles were characterized conductimetrically and potentiometrically by the manufacturer.

3.2. Apparatus

An Ecochemie Autolab PGSTAT12 potentiostat was used in conjunction with a Metrohm 663VA stand. The electrometer input impedance of this instrument is larger than 100 GΩ. The working electrode was a Metrohm multimode mercury drop electrode (surface area, 4.0×10^{-7} m^2, Merck mercury p.a.). The auxiliary electrode was glassy carbon and the reference electrode was a saturated calomel electrode, encased in a 0.1 M NaNO$_3$ salt bridge. Measurements were performed at 25 °C in a reaction vessel thermostated via a Lauda E100 unit. Proton titration experiments were performed using a computer controlled titration stand [19]. The pH was read using two pH electrodes and the reference electrode was a Ag|AgCl|KCl (3 M), encased in a 0.01 M KNO$_3$ jacket.

3.3. Electrochemical parameters

After the accumulation step an oxidizing strip current, I_s, of 1×10^{-9} A was applied in quiescent solution until the potential reached a value well passed the transition plateau. The I_s values used correspond to conditions approaching complete depletion ($I\tau$ constant). The SSCP waves were constructed from a series of measurements made over a range of deposition potentials, E_d. The potential was held at E_d for a deposition time, t_d, of 90 s, after which time the oxidizing current was applied.

4. Results and discussion

4.1. Lability criterion for steady-state convective diffusion

The electrochemical lability criterion for a spherical electrode and convective diffusion can be obtained from the analysis of the general steady-state metal flux to the electrode. This incorporates the mass transport as well as the complex formation/dissociation kinetics [11,12]

$$\frac{I_d^*}{nFA} = J^* = \frac{\overline{D}c_M^*(1 + K')}{\overline{d}}\left(1 + \frac{\mu\varepsilon K'}{\overline{d}}\right)^{-1} \qquad (13)$$

As outlined in Section 2.1, the two limiting cases for a dynamic system, labile and non-labile behavior, arise when the overall flux, J^*, is limited by diffusion or by the rate of complex dissociation, respectively. The lability criterion, L^* (where the asterisk has the same meaning as in $k_a^{*'}$) can be recognized as the term between brackets in Eq. (13)

$$L^* = \overline{d}/(\mu\varepsilon K')\begin{cases} \gg 1 & \text{labile} \\ \ll 1 & \text{non-labile} \end{cases} \qquad (14)$$

For the labile case the flux becomes J_{dif}^*

$$J_{dif}^* = \overline{D}C_{M,T}^*/\overline{d} \quad \text{(labile)} \qquad (15)$$

and for the non-labile case (assuming $\varepsilon K' \gg 1$) it becomes J_{kin}^*

$$J_{kin}^* = \frac{D_M C_M^*}{\mu} = k_d^*(D_M/k_a^{*'})^{1/2}C_{ML}^* \quad \text{(non-labile)} \qquad (16)$$

4.2. Experimental verification of the lability criterion

To validate this lability expression we compare L^* to the values obtained by SSCP measurements on metal ion/carboxylated latex nanospheres systems. More specifically we shall check if the experimental results follow the predicted dependence on the parameters in Eq. (3), i.e., the particle radius, a, the ligand concentration, C_L, and the particle concentration, c_p. The k_a value, as defined by k_{-w} and K_{os} is effectively a constant for a given metal ion, ligand charge, and ionic strength of the solution [13].

4.2.1. Influence of C_L and c_p

The ligand concentration C_L and the particle concentration c_p are related through the surface ligand concentration Γ_L

$$\Gamma_L = C_L/(4\pi a^2 c_p) \qquad (17)$$

Eq. (3a) can thus be rewritten in terms of Γ_L

$$k_a^{*'} = k_a'/(1 + k_a a\Gamma_L/D_M) \qquad (18)$$

The ligand concentration (C_L) can be changed either by (i) changing the particle concentration, where its variation is coupled with c_p while the surface concentration Γ_L remains constant, or (ii) changing the pH, thus changing the degree of protonation of the binding sites on the colloidal particle. The latter option comes to effectively increasing C_L and Γ_L, while maintaining c_p constant. Fig. 1 compares the variation of L^* with C_L for Pb(II) binding by latex particles (40 nm radius) as prescribed by Eq. (16) with the corresponding analogous homogeneous ligand solution for the same mobility of the complex species. In all cases the predicted lability of the colloidal dispersion is significantly less than that for the corresponding homo-
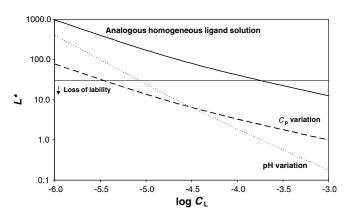

Fig. 1. Variation of the lability criterion, L^*, with ligand concentration, C_L (mol m^{-3}) for Pb(II) interaction with colloidal ligand dispersions of 40 nm radius particles and the analogous homogeneous ligand solution (solid line) for c_p variation (dashed line) ($\Gamma_L = 1.5 \times 10^{-7}$ mol m^{-2}) and pH variation (dotted line) ($c_p = 1.07 \times 10^{19}$ m^{-3}). Other parameters: $I = 0.01$ M, $d_M = 2.5 \times 10^{-5}$ m, $K = 10^7$ M^{-1}, $D_{Pb} = 9.9 \times 10^{-10}$ m^2 s^{-1}, $k_{-w(Pb)} = 7 \times 10^9$ s^{-1}, $K_{os} = 3.66 \times 10^{-3}$ mol^{-1} m^3 ($z_M z_L = -2$).

geneous case. Fig. 1 highlights an interesting feature of metal complexation by colloidal dispersions: the decrease in lability with increasing C_L is dependent on the manner in which the ligand concentration is varied. An increase in C_L invoked by an increase in pH induces a reduction in L^* greater than that due to the same change in C_L realized via an increase in c_p. The explanation of this feature lies in inspection of Eq. (18): on increasing the pH, Γ_L increases, and thus k_a^* decreases, whereas if c_p is increased both Γ_L and k_a^* remain constant and the change in lability parallels that of the corresponding homogeneous solution. The distinction between pH and c_p-controlled variation of C_L is a fundamental characteristic of colloidal ligand systems. It is an important practical consideration for interpretation of metal binding by colloidal ligands, and a useful diagnostic tool.

To decide whether variation of C_L by changing c_p or by changing pH is preferable for determination of the dynamic metal complexation parameters, we must identify the key experimental limitations in SSCP regarding the determination of the thickness of the reaction layer, μ. The determination of μ requires that the colloidal metal complexes must be quasi- or non-labile. In this situation the SSCP signal is lower than the corresponding signal for the labile case. Thus to minimize the loss of signal on increasing C_L, an increase of c_p at constant pH is preferable. This also has the advantage that the K value will be constant; for polyelectrolytic ligands the apparent K is likely to be dependent on the degree of ligand protonation, i.e., on pH.

Fig. 2a and b show the comparison between the experimentally determined and the calculated values of the lability parameter, L^*, as a function of C_L for lead(II) binding by 40 and 129 nm radius latex particles, respectively. There is a gratifying agreement for the 40 nm particles. The results obtained for the 129 nm particles are very near the
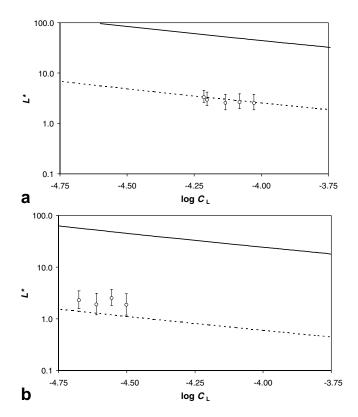
a

b

Fig. 2. Experimental verification of the dependence of the lability criterion, L^*, on the ligand concentration, C_L (mol m^{-3}) ($\Gamma_L = 2.8 \times 10^{-7}$ mol m^{-2}) for Pb(II) interaction with: (a) Carboxylated latex particles of 40 nm radius. Other parameters: $I = 0.01$ M, pH 6.7, $d_M = 4.0 \times 10^{-5}$ m, $K = 1.46 \times 10^7$ M^{-1}, $D_{Pb} = 9.9 \times 10^{-10}$ m^2 s^{-1}, $k_{-w(Pb)} = 7 \times 10^9$ s^{-1}, $K_{os} = 3.66 \times 10^{-3}$ mol^{-1} m^3 ($z_M z_L = -2$). (b) Carboxylated latex particles of 129 nm radius. Other parameters: $I = 0.01$ M, pH 6.4, $d_M = 5.7 \times 10^{-5}$ m, $K = 9.33 \times 10^7$ M^{-1}, $D_{Pb} = 9.9 \times 10^{-10}$ m^2 s^{-1}, $k_{-w(Pb)} = 7 \times 10^9$ s^{-1}, $K_{os} = 3.66 \times 10^{-3}$ mol^{-1} m^3 ($z_M z_L = -2$). Experimental data (O), calculated from dynamic colloidal theory (dashed line) and for the analogous homogeneous ligand solution (solid line).

detection limit of the technique ($\tau_{M+L}^* \approx 1$ s), due to the low mobility ($D_{ML} = 1.73 \times 10^{-12}$ m^2 s^{-1}) and the quasi-labile character of the complexes. The evidence is still convincing since the measured values are some 30 times lower than those predicted for the analogous homogeneous case.

4.2.2. Influence of particle radius

Increasing the particle radius, a, while keeping the ligand concentration (C_L) constant, implies that the number of particles c_p must decrease accordingly. It also implies a decrease in D_{ML}, meaning that in the calculation of the analogous homogeneous solution we consider the ligands to be homogeneously distributed over the solution volume with a mobility equal to that of the colloidal ligands in the dispersion [7]. Fig. 3 compares the theoretical dependence of the lability criterion (L^*) on the particle radius, a, for colloidal ligand dispersions with that for the analogous homogeneous ligand solution. By keeping C_L constant, the surface concentration Γ_L changes, hence the observed variations in L^* are effectively due to changes in $a\Gamma_L$ (Eq. (18)). As
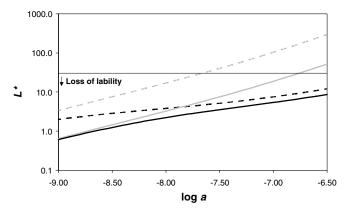

Fig. 3. Theoretical variation of the lability criterion, L^*, with particle radius, a (m), for the dynamic theory for colloidal ligand dispersions (black lines) and the analogous homogeneous ligand solution (grey lines), for Pb(II) (dashed line) and Cd(II) (full line) in the presence of $C_L = 10 \times 10^{-3}$ mol m^{-3} binding sites. Other parameters: $I = 0.01$ M, $d_M = 3.0 \times 10^{-5}$ m, $K = 1 \times 10^7$ M^{-1}, $D_{Pb} = 9.9 \times 10^{-10}$ m^2 s^{-1}, $D_{Cd} = 7.0 \times 10^{-10}$ m^2 s^{-1}, $k_{-w(Pb)} = 7 \times 10^9$ s^{-1}, $k_{-w(Cd)} = 3 \times 10^8$ s^{-1}, $K_{os} = 3.66 \times 10^{-3}$ mol^{-1} m^3 ($z_M z_L = -2$).

observed before for the diffusion-controlled techniques [7], the increase in lability of colloidal metal complexes with increasing a is significantly toned down as compared with the analogous homogeneous ligand solution. This effect is more important for Pb(II) than for Cd(II) due to the higher k_a of the former.

Fig. 3 does not include experimental data due to the difficulty in obtaining fully comparable results for the different particle radii. This arises from the surface concentration Γ_L dependency on the particle radius (Eq. (17)). Therefore, we present the experimental and corresponding theoretical values in Table 1. Consistent with the results presented above for the variation of C_L, the experimental values of the lability parameter agree quite well with the predicted ones and are significantly smaller than those for the analogous homogeneous solution.

The values of K' and C_L are different for each particle and this makes the lability comparison more involved. Nonetheless it can be seen that for Pb(II) an increase of the particle radius from 15 nm (line 3) to 40 nm (line 5) results in an experimental increase of L^* from 0.7 to 2.6, almost identical to the calculated increase from 0.7 to 2.7, but much smaller than the increase from 2.3 to 46 for the analogous homogeneous ligand solution.

Further developments will require the investigation of the polyelectrolytic effect on the stability constant and its effect on the lability of metal complexes in colloidal ligand dispersions. A rough estimate provides a separation between charges of about 1.5 nm for our fully deprotonated systems. This clearly suggests that understanding the coupling of changes of ligand concentration due to variation of pH with polyelectrolytic counterion binding effects is fundamental in the understanding of the dynamic behavior of trace metals in natural waters, especially those with low ionic strength and/or variable pH.

Table 1
Influence of the radius in the lability for lead and cadmium nanosphere systems at ionic strength 0.01 M

$a/10^{-9}$ m	$C_L/10^{-3}$ mol m^{-3}	ε	$K'(\Delta E_{d,1/2})/10^2$	$\mu/10^{-6}$ m	$d_M/10^{-6}$ m	$\bar{d}/10^{-6}$ m	$k_a C_L$ (exp)$/10^3$ s^{-1}	$k_a C_L$ (Eigen)$/10^3$ s^{-1}	$k_a^* C_L/10^3$ s^{-1}	L^* exp	L Eigen	L^*
Pb												
15.0	3.3	0.015	3.2 ± 0.2	0.35	13.8	3.9	7.9 ± 3.9	82.6	10.8	2.3 ± 0.6	6.7	2.7
15.0	4.3	0.015	11.0 ± 0.9	0.33	24.7	7.0	9.2 ± 3.1	106.5	11.2	1.3 ± 0.2	4.3	1.4
15.0	4.4	0.015	11.1 ± 0.8	0.30	13.8	3.7	10.6 ± 4.1	106.5	11.2	0.7 ± 0.1	2.3	0.7
40.0	60.6	0.0057	2.7 ± 0.20	0.45	41.5	10.7	4.8 [2.2–13]	1575	5.3	10–25	277	16.1
40.0	94.1	0.0057	13.3 ± 0.20	0.37	32.8	7.2	7.4 ± 1.5	2445	8.1	2.6 ± 0.3	46	2.7
60.5	21.7	0.0037	0.48 ± 0.04	0.72	13.3	4.1	0.9 [0.2–16]	555	0.76	10–93	553	20.3
60.5	58.8	0.0037	0.78 ± 0.03	0.77	15.7	4.2	1.6 [0.4–5.2]	1502	2.1	9–33	580	21.2
60.5	65.0	0.0037	2.6 ± 0.2	0.78	15.7	3.3	1.6 ± 0.7	1665	2.1	4.4 ± 1.0	142	5.0
129.0	30.0	0.0018	7.4 ± 0.5	0.89	39.6	7.1	1.2 ± 0.7	798	0.50	5.9 ± 1.8	153	3.8
129.0	31.4	0.0018	22 ± 3	0.72	39.6	6.4	1.9 ± 0.9	822	0.51	2.2 ± 0.5	49	1.2
Cd												
15.0	27.5	0.021	18.4 ± 1.5	0.30	32.6	10.5	8.0 ± 2.5	30.3	6.7	0.7 ± 0.1	1.8	0.8
60.5	107.0	0.0053	0.64 ± 0.03	0.88	23.7	7.2	0.9 [0.16–38]	118	2.2	9–132	282	53.9
60.5	118.0	0.0053	1.13 ± 0.04	0.86	23.7	6.3	0.95 [0.3–19]	130	1.6	6–46	147	22.8

5. Conclusions

A lability criterion has been formulated for colloidal metal complexes in stirred solutions where convective diffusion is the dominant mode of mass transport. The predicted values for colloidal complexes of Pb(II) and Cd(II) in carboxyl modified latex dispersions, and their dependence on ligand concentration and particle radius, are in good agreement with experimental data. In colloidal ligand dispersions the observed increase in lability with increasing particle radius is significantly toned down as compared with the analogous homogeneous ligand solution, in accord with earlier predictions [7].

The conventional approach of assuming a smeared-out ligand distribution overestimates the lability of a colloidal ligand system. The dependence of lability on the variation of C_L depends strongly on the way in which this parameter is manipulated: a pH increase invokes a greater loss of lability than does an increase in c_p. This feature is characteristic of the spatial distribution of the sites in a colloidal dispersion and is therefore fundamental to interpretation of metal speciation in such systems.

Acknowledgments

References

[1] J.P. Pinheiro, M. Minor, H.P. van Leeuwen, Langmuir 21 (2005) 8635.
[2] W. Davison, J. Electroanal. Chem. 87 (1978) 395.
[3] H.P. van Leeuwen, J. Buffle, R. Cleven, Pure Appl. Chem. 61 (1989) 255.
[4] J. Galceran, J. Puy, J. Salvador, J. Cecilia, H.P. van Leeuwen, J. Electroanal. Chem. 505 (2001) 85.
[5] J. Buffle, K.J. Wilkinson, S. Stoll, M. Filella, J. Zhang, Environ. Sci. Technol. 32 (1998) 2887.
[6] A.M. Mota, M.M. Correia dos Santos, in: A. Tessier, D. Turner (Eds.), Metal Speciation and Bioavailability, John Wiley & Sons, New York, 1995 (Chapter 5).
[7] J.P. Pinheiro, M. Minor, H.P. van Leeuwen, J. Electroanal. Chem. 587 (2006) 284.
[8] R.M. Town, H.P. van Leeuwen, J. Electroanal. Chem. 523 (2002) 1.
[9] R.M. Town, H.P. van Leeuwen, J. Electroanal. Chem. 541 (2003) 51.
[10] H.P. van Leeuwen, R.M. Town, Environ. Sci. Technol. 37 (2003) 3945.
[11] H.P. van Leeuwen, R.M. Town, J. Electroanal. Chem. 561 (2004) 67.
[12] J.P. Pinheiro, H.P. van Leeuwen, J. Electroanal. Chem. 570 (2004) 69.

[13] F.M.M. Morel, J.G. Hering, Principles and Applications of Aquatic Chemistry, John Wiley, New York, 1993.

[14] H.P. van Leeuwen, Electroanalysis 13 (2001) 826.

[15] H.P. van Leeuwen, R.M. Town, J. Electroanal. Chem. 536 (2002) 129.

[16] J. Heyrovský, J. Kůta, Principles of Polarography, Publishing House of the Czechoslovak Academy of Sciences, Praha, and Academic Press, New York, 1966.

[17] V.G. Levich, Physicochemical Hydrodynamics, Prentice-Hall, Englewood Cliffs, NJ, 1962.

[18] M.C. Wilkinson, J. Hearn, P.A. Steward, Adv. Coll. Int. Sci. 81 (1999) 77.

[19] D.G. Kinniburgh, C.J. Milne, P. Venema, Soil Sci. Am. J. 59 (1995) 417.